

A System for Endoscopic Submucosal Dissection Featuring Concentric Push-Pull Manipulators

Peter Connor¹, Carter Hatch², Khoa Dang², Tony Qin³, Ron Alterovitz³, Caleb Rucker², Robert J. Webster III¹

Abstract—Endoscopic Submucosal Dissection (ESD) is an effective minimally invasive approach to removing colon cancer, yet it is underutilized, since it is challenging to learn and perform. To promote the adoption of ESD by making it easier, we propose a system in which two small, flexible robotic manipulators are delivered through a colonoscope. Our system differs from prior robotic systems aimed at this application in that our manipulators are small enough to fit through a clinically used colonoscope. By not re-engineering the colonoscope, we maintain overall system diameter at the eventual clinical gold standard, and streamline the path to eventual clinical deployment. Our concentric push-pull robot (CPPR) manipulators offer dexterity and simultaneously provide a conduit for grasper or cutting tool deployment. Each manipulator in our system consists of two push-pull tube pairs, and we describe how they are actuated. We describe for the first time our approach to compensating for undesirable CPPR tip motion induced by differences in the tubes’ transmission stiffness. We also evaluate the workspace of the manipulators and demonstrate teleoperation in a point-touching experiment. Lastly, we demonstrate the ability of the system to resect tissue via ex vivo animal experiments.

I. INTRODUCTION

Despite the benefits of endoscopic procedures in colon cancer removal, widespread adoption is limited by the limited dexterity of current tools, which makes these procedures challenging to perform [1]. Among these procedures is Endoscopic Submucosal Dissection (ESD), in which an endoscope is used to remove colorectal cancer [2]. ESD has been shown to have many advantages over traditional surgical options including a lower recurrence rate, lower mortality rate, and higher patient quality of life [3]. However, ESD remains highly underutilized due to how challenging it is to learn and perform [3].

The typical approach to ESD is to perform it with tools that extend axially through the endoscope tool ports, and the tools are unable to controllably move off of the port axis. The only way the surgeon can aim these tools is to curve

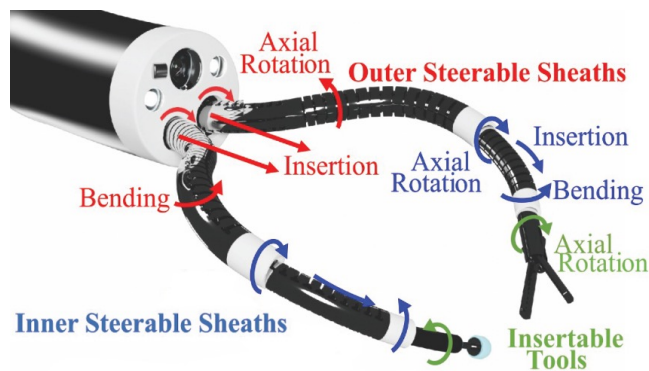


Fig. 1. Our system provides two arms, each made from two, two-tube concentric push pull robots. Each pair of tubes is capable of insertion, axial rotation, and bending independent of the other pairs.

the entire endoscope tip, which also moves the surgeon’s viewpoint. This can be disorienting for the surgeon [4]. Furthermore, if more than one tool is present (which is typically true; surgeons use dual-channel endoscopes), tools move in a coupled manner. This makes it impossible to apply controlled tension to tissue to facilitate cutting. Such tension is referred to as “countertraction,” and is known to improve the cutting process [5].

Motivated by these factors, prior researchers have sought to develop robotic systems for ESD [6]. For example, the MASTER system is a linkage-based 10 degree of freedom (DoF) bimanual system [7], [8]. The STRAS system [9]–[11] is a bimanual system developed as a later version of Anubiscope (Karl Storz Endoskope). This robot has 10 DoF and uses a custom flexible endoscope. The FLEX Robotic System (Medrobotics Corporation) is a dexterous system with a custom endoscope that can reach 25 cm from the anal verge to perform ESD in the colon [4]. DREAMS is a tendon-driven flexible parallel continuum wrist system developed for ESD [12]. Other systems also seek to add dexterity to flexible endoscopic procedures, such as the K-Flex System [13], the Endoluminal Surgical System [14], and REXTER [15].

All of these systems developed for robotically assisted ESD require larger, custom endoscopes, or exterior attachments to the endoscope. The clinical feasibility of increasing the size of and/or changing the shape of the endoscope is unclear, and doing so certainly presents higher regulatory burden and potentially adds cost to the overall system.

¹Peter Connor and Robert J. Webster III are with Vanderbilt University Department of Mechanical Engineering.

²Khoa Dang, Carter Hatch, and Caleb Rucker are with The University of Tennessee, Knoxville, Department of Mechanical, Aerospace, and Biomedical Engineering.

³Tony Qin and Ron Alterovitz are with the University of North Carolina at Chapel Hill, Department of Computer Science.

This work is supported by National Institute of Biomedical Imaging and Bioengineering of the National Institutes of Health (NIH) under award number R01EB032385. Any opinion, findings, and conclusions or recommendations expressed herein are those of the authors and do not necessarily reflect the views of the NIH.

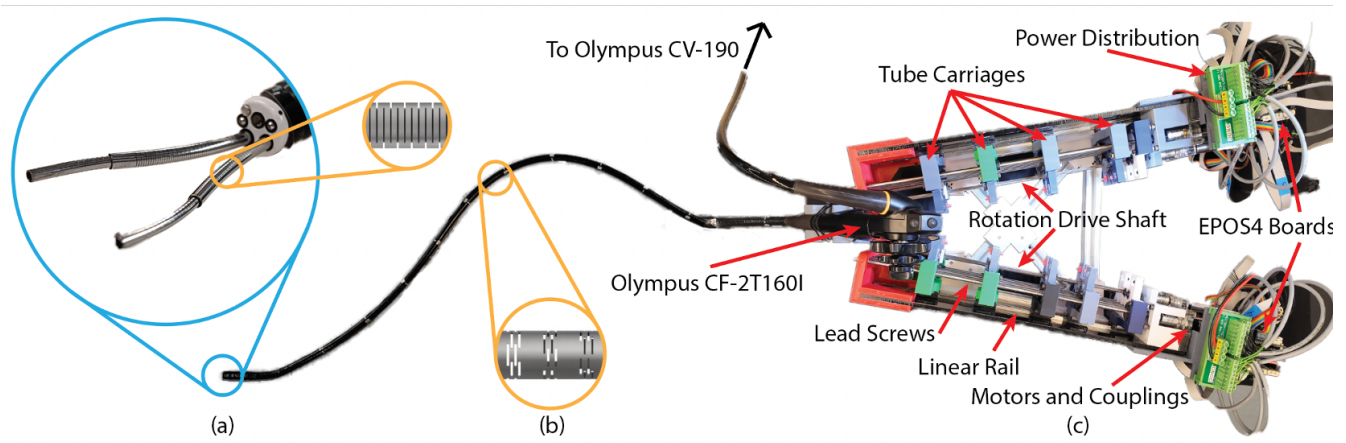


Fig. 2. Overview of the main components of the system: (a) the dexterous push-pull robotic tools, (b) transmission segment of the tubes passing through a standard clinical colonoscope, and (c) the actuation unit to drive the system

Based on these factors, we seek to create a system that uses only an unmodified clinical endoscope with robotic tools passed through its existing ports. Concentric push-pull robots (CPPRs) [16] provide a means of making steerable sheaths so small and thin-walled that they can pass through existing colonoscope ports and still carry standard transendoscopic tools through themselves. CPPRs are constructed from one or more pairs of thin-walled tubes that are attached at their tips, with each having material systematically removed (typically by laser micromachining) to enable desired dexterity profiles.

Previous research produced mechanics-based models for constant [17] and variable curvature [16] CPPRs, which can be used to design robots with desired bending capabilities. Slot self-contact has also been included in models to define pre-set maximum curvatures [18], and the effects of external loads have also been modeled [19]. These foundational models set the stage for the work in this paper, which is the first to describe a complete teleoperated, bimanual system featuring colonoscope-deployed concentric push-pull manipulators, and to experimentally demonstrate animal tissue resection using it.

II. SYSTEM DESIGN AND ACTUATION

Our system concept is as shown in Fig. 1. Each manipulator consists of two nested push-pull tube pairs. The inner push-pull pair and the outer push-pull pair can be inserted, bent, and rotated independently. This provides 6 DoF for each manipulator plus any end effector degrees of freedom (e.g., axial tool rotation). The primary, though not only, function of the outer tube pair is to provide instrument triangulation (i.e., push tubes outward from the camera so the axes of the tools and camera are not roughly aligned). We also designed our system to facilitate rapid intraprocedural tool changes.

A. Endoscope Parameters

We use the CF-2T160I from Olympus, a clinical colonoscope that provides two ports through which we can pass our manipulators. It has a total length of 1500 mm from the tool

entrance to the distal tip and two channels with diameters of 3.7 mm and 3.2 mm. While there is no fundamental limit to how far the endoscope can see, we have observed that objects are difficult to illuminate and see clearly beyond approximately 56 mm from the endoscope's tip, so we set this as the boundary of the viewable area in this paper. Additionally, we define the field of view (FOV) of our endoscope as the minimum angle of the ray that passes from the endoscope to the edge of the view area, which is 100 degrees for our endoscope.

B. Actuation System

The actuation system consists of two mirrored actuation units, with each capable of driving two, two-tube concentric push-pull manipulators. These actuation units are inspired by the design presented for steerable needles in [20]. A major advantage of this design is that it facilitates quick intraprocedural tool changes. The actuation unit for each manipulator has 5 lead screws driven by rear-mounted motors (Maxon 283835 driven by Maxon EPOS4 Digital Positioning Controllers) which independently control the insertion of each tube and the tool that passes through it. Each is driven by a tube carriage supported by a linear rail and ball bearing slide. Because axial rotation of the tubes in a pair should always be identical in the case of CPPRs, rotation is driven by a keyed shaft passing through both carriages. This improvement on prior designs ensures the synchronization of pair rotation.

Because surgeons may need to use multiple tools through the course of a procedure, our actuation unit also accommodates tool changes. We do this via a modification to the mechanism in [20] that accounts for the larger axial loads required for CPPRs than for the steerable needles considered in that work. Our quick-release mechanism is as shown in Fig. 3. In [20], the removable tube housing is axially constrained by a small plate partially covering the housing gear and fixed within the carriage by spring-loaded rollers. When subjected to the axial loads of CPPRs, the tube housing can twist out of the rollers, losing contact with the carriage.

To address this, we designed axial guides into the carriage itself which span the height of the removable tube holder, which prevents the twisting motion. Meanwhile, a spring-loaded latch ensures proper meshing of the gears when a tube is inserted. The mechanism also provides switches that enable a tube pair to be easily removed and replaced. The tubes are held in place axially and torsionally with an SDP-SI Shaftloc clamp which applies radial pressure to both the tube and the supporting gear to eliminate relative motion. The gears are doubly supported by ball bearings and axially constrained by a snap ring.

C. Tube Transmission Design and Stretch Compensation

The transmission sections of the tubes are the portions that pass through the endoscope and connect the actuation unit to the bendable manipulators that extend from the tip of the endoscope. We described the design of these laser-machined transmission sections in [21]. There, the general goals were to have high axial and torsional stiffness, with bending stiffness low enough that it does not negatively affect the performance of the colonoscope.

Even in well-designed transmission sections, there will be significant axial stretch and compression during actuation, which must be compensated for in order to control bending at the tip. Toward compensating for axial stretch, we experimentally measured the relationship between the relative displacement at the bases of an attached pair of CPPR tubes ($q_2 - q_1$) and bending angle of the steerable section when fully extended from the endoscope tip. We measured tip angle using a NDI Aurora Electromagnetic Tracker while applying relative displacement of the tube bases in increments of 2 mm. The results are shown in Fig. 4. We fit a line to the portions of this data before notch closure begins. The equation of this line gives the relationship between actuator displacement and bending angle of the steerable tip, including transmission effects:

$$q_2 - q_1 = C\theta,$$

where θ is the angle of the tip of the CPPR pair, and $C = 26.04$ mm/rad is fit from the data.

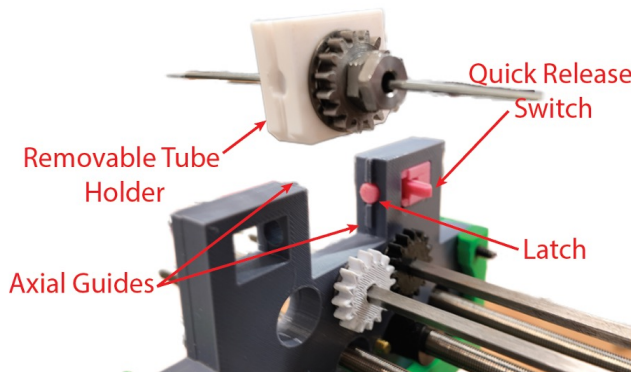


Fig. 3. A removable tube holder can be inserted locked into the carriage. This mechanism facilitates easy insertion and removal of the bases of the CPPRs from their respective carriages in the actuation unit.

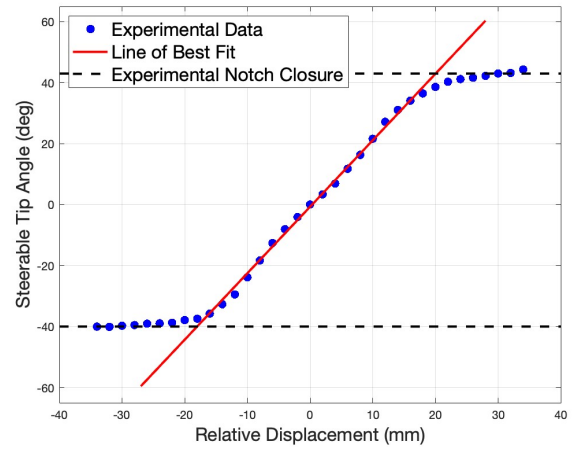


Fig. 4. Experimental results for the relative displacement of the tube bases vs. the angle of the steerable tip. The tubes reach experimental notch closure at around 42 degrees.

Since the inner and outer tubes will differ in axial stiffness, the elongation and shortening of each tube during differential tube actuation will also differ. Our goal is to compensate for these transmission elongations in order to satisfy a desired bending angle θ , without allowing unintended net elongation (or shortening) of the CPPR tube pair to move the tip axially.

The magnitude of the compensation to be applied can be determined from the ratio of tube transmission stiffnesses. Because the force through all tubes is assumed to be constant¹ and the transmission behaves as a linear spring, Hooke's Law applies to all segments of the tube pair:

$$\tau = k_a(q_2 - q_1) = k_a C\theta = k_1\delta_1 = -k_2\delta_2,$$

where the subscripts 1 and 2 refer to the outer and inner tube, respectively, τ is the actuation force, k_a is the stiffness seen by the actuation system, and δ_i is the elongation of transmission tube i . δ_2 contains a negative term because a pushing motion in the inner tube ($q_2 > q_1$) causes a shortening of the inner tube. It follows that the elongation of each transmission tube can be found using:

$$\delta_1 = \frac{k_a}{k_1} C\theta \quad \delta_2 = -\frac{k_a}{k_2} C\theta$$

k_a can be physically calibrated by measuring the relationship between τ and $(q_2 - q_1)$ and using a linear regression to estimate the slope. k_1 and k_2 can be estimated either using finite element analysis [21] or by physical calibration similar to k_a . We calibrated both k_a and k_1 using a force sensor (ATI Mini-40 SI-40-2) and a manual linear actuator. For the outer pair of the larger arm, this best fit gives $k_a = 0.24$ N/mm and $k_1 = 0.405$ N/mm. Thus, during bending actuation, if we want the base of the outer tube bending segment to remain stationary, we must move q_1 by $-\delta_1$, and move q_2 by $C\theta - \delta_1$, while insertion of the entire segment is achieved by moving q_1 and q_2 identical amounts in the same direction.

¹Note that friction between tubes is assumed to be small in prior models and this has been experimentally validated [19].

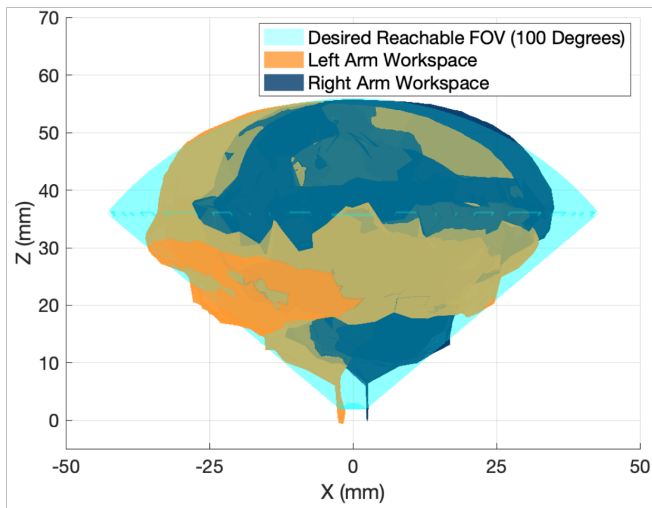


Fig. 5. Results of the magnetically tracked workspace of the robot compared to the endoscope FOV.

III. TUBE SELECTION AND WORKSPACE

CPPRs have many design parameters, and when one considers two nested CPPR tube pairs, additional parameters such as the arc lengths and the curvatures of each pair can also be considered. Within this large dimensional space, our general goals in choosing parameters are to reach where the endoscope can see and provide good dexterity and triangulation. Using computational simulations of the robot's workspace [22], we explored maximum curvatures and arc lengths of the two CPPRs in a given manipulator to satisfy these goals. We selected an outer tube pair maximum curvature of 0.035 mm^{-1} and arc length of 30 mm, and an inner tube maximum curvature of 0.1 mm^{-1} and arc length of 16 mm, which qualitatively satisfied these objectives, as can be seen in Fig. 5. We also note that we provide a 5mm straight uncut tip section on each tube to facilitate laser welding.

The tubes were fabricated to have an Outer Diameter/Inner Diameter ratio of 1.08. The radial clearance was selected to be 0.1 mm to enable smooth push-pull operation. Based on this and the scope specifications in section II-A, the tube dimensions used for each arm are given in Table I. Tubes 1-4 are used in Arm 1 (which passes through the 3.7 mm diameter tool port) and tubes 2-5 are used in Arm 2 (which passes through the 3.2 mm diameter tool port). A constant curvature single serpentine beam element pattern was used to achieve the desired lengths and maximum curvatures [18], using laser kerf width cuts. The theoretical actuation forces, based on the validated tube model in [16], for each pair ranges from 4.8 N for the largest manipulator to 6.1 N for the smallest manipulator, which are easily achievable actuation forces for our system. A full set of eight Nitinol tubes was manufactured through femtosecond laser cutting (Peierltech, China).

To experimentally evaluate the workspace of the system, we attached magnetic tracking coils to the manipulator tips. With the manipulators deployed through the colonoscope, we



Fig. 6. Experimental setup for workspace validation. Both arms were swept between the joint limits while outfitted with a magnetic tracker on the tip.

actuated the tubes to sweep the workspace. The experimental setup is shown in Fig. 6.

The data for both arms are plotted (using MATLAB's AlphaShape function) in Fig. 5 and overlaid onto the desired workspace based on the endoscope's FOV as discussed in Section II-A.

IV. TELEOPERATION

To provide a surgeon control interface, we use 3DSys-tems Touch Haptic Devices, shown in Fig. 7. Teleoperation was implemented using ROS Noetic. The system provides clutching through a button press on the Touch controller. We implemented a modified version of the redundancy resolution algorithm presented in [23] to enable teleoperation. The algorithm moves the robot at each time step a distance along the kinematic twist that will reduce the error between current and desired position. In addition to reducing this error, the algorithm seeks to minimize an objective function that combines a variety of control objectives with various weights. In our case, the objective function seeks to track the desired trajectory towards a target point while damping the joints and avoiding joint limits. Compared to [23], we do not require a stability-aware term in our objective function, so we exclude the secondary objective function and instead take a damped least squared solution to the inverse kinematics using only tracking, joint damping, and joint limit avoidance.

To evaluate teleoperation, we conducted the following experiment. We created a 20 mm diameter hemisphere

TABLE I
TUBE DIMENSIONS

	OD (mm)	ID (mm)	Arm 1	Arm 2
Tube 1	3.3	3.04	●	
Tube 2	2.84	2.62	●	●
Tube 3	2.42	2.24	○	●
Tube 4	2.04	1.88	○	○
Tube 5	1.68	1.54		○

- : tube is a member of the outer pair.
- : tube is a member of the inner pair



Fig. 7. Example setup of a surgeon control interface for bimanual operation of the endoscopic system



Fig. 8. Setup for the robot to do the point touching experiment

(roughly representing a tumor the robot might be tasked with removing) with contact points distributed on the surface. The contact points on the quarter sphere facing the scope were set as targets for the user to touch, in random order. When the electrical circuit is closed by the user touching one of these (with either arm), the point is considered touched, and a new contact point becomes the target, until all points have been reached. We found that the user was able to teleoperate the robot to all points using the 3D Systems Touch Haptic Devices. The setup for the robot performing this point touching test is shown in Fig. 8.

V. EX VIVO EXPERIMENTS

Lastly, we explored the system’s ability to endoscopically resect tissue. The robotic arms with attached actuation unit were passed through an Olympus CF-2T160I Colonoscope which was attached to an Olympus CLV-190 and CV-190 for illumination and video feed recording.

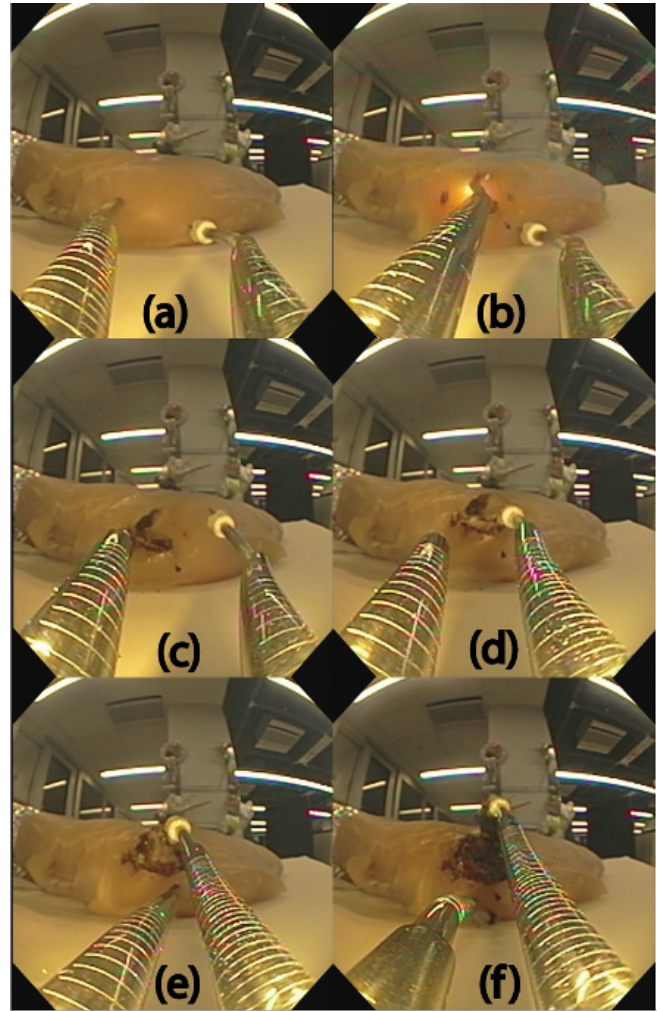


Fig. 9. Results from the chicken breast resection experiment (a) Endoscopic view before resection begins (b) marking the boundary to resect (c) initial cuts (d-e) countertraction of tissue to continue resection (f) tissue after the resection.

The right arm was equipped with a small pointed instrument for tissue manipulation and the left arm was equipped with a modified electrocautery tool for cutting. A chicken breast was secured within the endoscope FOV and the workspace of the robot. The manipulators were used to mark a perimeter for removal and resect the target tissue, using countertraction to manipulate the tissue as needed. Endoscopic images from the chicken breast resection process are shown in Fig. 9. In (d), (e), and (f), the right arm can be seen applying countertraction to the tissue while the left arm continues cutting the newly exposed surface.

VI. CONCLUSIONS

In this paper, we propose the first integrated, bimanual, multi-segment concentric push-pull robot for deployment through a commercial colonoscope. We described the endoscope, actuation unit, tube sets, and our teleoperation approach. We experimentally evaluated the workspace of the robot showing that it can reach approximately everywhere it can see, that a user can effectively teleoperate the robot, and

that it can be used to remove tissue from a chicken breast. We also identified the need for actuation compensation, since the two tubes in a given pair will nearly always have different transmission stiffnesses which will lead to unplanned axial tip motion, without the compensation approach we proposed herein.

An important area for future research will be computational optimization of the many parameters afforded by CPPRs. This optimization can take into account factors such as dexterity, stiffness, actuation loads, and the cutting options afforded by laser micromachining. Fortunately, even without optimization the first tube set we made for this system, which we described in this paper, was able to reach nearly all of the volume the endoscope can view, and provided useful dexterity and triangulation.

Another area for future research will be to characterize the stiffness and retraction capabilities of our manipulators in various directions, at various workspace locations. The forces required for our chicken breast experiments seem to us to generally correspond to what would be needed from the manipulators in ESD, but this remains to be experimentally demonstrated in colon experiments. Furthermore, it will be useful to both theoretically and experimentally characterize the stiffness of specific manipulator prototypes in the future, to better understand their maximum load bearing capabilities.

In summary, we believe that the type of system we have proposed in this paper has the potential to one day make ESD easier to perform. It also has the potential to reach clinical use more rapidly, and potentially less expensively, than prior systems that re-design the endoscope. If we are successful in bringing such a device to market and proving our hypothesis that it makes ESD easier to perform, we will be well on our way to our ultimate goal of bringing the known clinical benefits of ESD to many more patients.

REFERENCES

- [1] M. Krantzfelder, A. Schneider, A. Fiolka, S. Koller, D. Wilhelm, S. Reiser, A. Meining, and H. Feussner, "What do we really need? visions of an ideal human-machine interface for NOTES mechatronic support systems from the view of surgeons, gastroenterologists, and medical engineers," *Surgical Innovation*, vol. 22, no. 4, pp. 432–440, 2015.
- [2] N. Matsui, "Endoscopic submucosal dissection for removal of superficial gastrointestinal neoplasms: A technical review," *World Journal of Gastrointestinal Endoscopy*, vol. 4, no. 4, p. 123, 2012.
- [3] P. V. Draganov, H. Aihara, M. S. Karasik, S. Ngamruengphong, A. A. Aadam, M. O. Othman, N. Sharma, I. S. Grimm, A. Rostom, B. J. Elmunzer, S. A. Jawaid, D. Westerveld, Y. B. Perbtani, B. J. Hoffman, A. Schlachterman, A. Siegel, R. M. Coman, A. Y. Wang, and D. Yang, "Endoscopic submucosal dissection in north america: A large prospective multicenter study," *Gastroenterology*, vol. 160, no. 7, pp. 2317–2327, 2021.
- [4] D. Turiani Hourneaux De Moura, H. Aihara, P. Jirapinyo, G. Farias, K. E. Hathorn, A. Bazarbashi, A. Sachdev, and C. C. Thompson, "Robot-assisted endoscopic submucosal dissection versus conventional ESD for colorectal lesions: outcomes of a randomized pilot study in endoscopists without prior ESD experience (with video)," *Gastrointestinal Endoscopy*, vol. 90, no. 2, pp. 290–298, 2019.
- [5] M. Nagata, "Advances in traction methods for endoscopic submucosal dissection: What is the best traction method and traction direction?" *World Journal of Gastroenterology*, 01 2022.
- [6] N. Tada and K. Sumiyama, "Robotic platforms for therapeutic flexible endoscopy: A literature review," *Diagnostics*, vol. 14, no. 6, p. 595, 2024.
- [7] S. J. Phee, S. C. Low, Z. L. Sun, K. Y. Ho, W. M. Huang, and Z. M. Thant, "Robotic system for no-scar gastrointestinal surgery," *The International Journal of Medical Robotics and Computer Assisted Surgery*, vol. 4, no. 1, pp. 15–22, 2008.
- [8] K.-Y. Ho, S. J. Phee, A. Shabbir, S. C. Low, V. A. Huynh, A. P. Kencana, K. Yang, D. Lomanto, B. Y. J. So, Y. J. Wong, and S. S. Chung, "Endoscopic submucosal dissection of gastric lesions by using a master and slave transluminal endoscopic robot (MASTER)," *Gastrointestinal Endoscopy*, vol. 72, no. 3, pp. 593–599, 2010.
- [9] L. Zorn, F. Nageotte, P. Zanne, A. Legner, B. Dallemagne, J. Marescaux, and M. De Mathelin, "A novel telemanipulated robotic assistant for surgical endoscopy: Preclinical application to ESD," *IEEE Trans. Biomed. Eng.*, vol. 65, no. 4, pp. 797–808, 2018.
- [10] B. Dallemagne and J. Marescaux, "The ANUBIS™ project," *Minimally Invasive Therapy & Allied Technologies*, vol. 19, no. 5, pp. 257–261, 2010.
- [11] A. Légnér, M. Diana, P. Halvax, Y.-Y. Liu, L. Zorn, P. Zanne, F. Nageotte, M. De Mathelin, B. Dallemagne, and J. Marescaux, "Endoluminal surgical triangulation 2.0: A novel flexible surgical robot. preliminary pre-clinical results with colonic submucosal dissection," *The International Journal of Medical Robotics and Computer Assisted Surgery*, vol. 13, no. 3, p. e1819, 2017.
- [12] H. Gao, X. Yang, X. Xiao, X. Zhu, T. Zhang, C. Hou, H. Liu, M. Q.-H. Meng, L. Sun, X. Zuo, Y. Li, and H. Ren, "Transendoscopic flexible parallel continuum robotic mechanism for bimanual endoscopic submucosal dissection," *The International Journal of Robotics Research*, vol. 43, no. 3, pp. 281–304, 2024.
- [13] M. Hwang and D.-S. Kwon, "K-FLEX: A flexible robotic platform for scar-free endoscopic surgery," *The International Journal of Medical Robotics and Computer Assisted Surgery*, vol. 16, no. 2, p. e2078, 2020.
- [14] S. Atallah, A. Sanchez, E. Bianchi, and S. W. Larach, "Envisioning the future of colorectal surgery: preclinical assessment and detailed description of an endoluminal robotic system (ColubrisMX ELS)," *Tech Coloproctol*, vol. 25, no. 11, pp. 1199–1207, 2021.
- [15] B. G. Kim, H. S. Choi, S. H. Park, J. H. Hong, J. M. Lee, S. H. Kim, H. J. Chun, D. Hong, and B. Keum, "A pilot study of endoscopic submucosal dissection using an endoscopic assistive robot in a porcine stomach model," *Gut Liver*, vol. 13, no. 4, pp. 402–408, 2019.
- [16] K. Oliver-Butler, J. A. Childs, A. Daniel, and D. C. Rucker, "Concentric push-pull robots: Planar modeling and design," *IEEE Trans. Robot.*, vol. 38, no. 2, pp. 1186–1200, 2022.
- [17] K. Oliver-Butler, Z. H. Epps, and D. C. Rucker, "Concentric agonist-antagonist robots for minimally invasive surgeries," in *SPIE Medical Imaging*, 2017.
- [18] J. Gafford, D. C. Rucker, P. L. Anderson, S. J. Webster, and R. J. Webster, "Agonist-antagonist tube steerable instrument with serpentine beam elements," patent WO2 023 076 667A1, 2022.
- [19] J. A. Childs and C. Rucker, "A kinetostatic model for concentric push-pull robots," *IEEE Trans. Robot.*, vol. 40, pp. 554–572, 2024.
- [20] S. Amack, M. Rox, J. Mitchell, T. E. Ertop, M. Emerson, A. Kuntz, F. Maldonado, J. Akulian, J. Gafford, R. Alterovitz, and R. J. Webster III, "Design and control of a compact, modular robot for transbronchial lung biopsy," in *SPIE Medical Imaging*, 2019.
- [21] K. T. Dang, S. Qiu, C. Hatch, P. Connor, T. Qin, R. Alterovitz, R. J. Webster III, and C. Rucker, "Design of transmission tubes for surgical concentric push-pull robots," in *2024 International Symposium on Medical Robotics (ISMR)*, 2024, pp. 1–7.
- [22] T. Qin, P. Connor, K. Dang, R. Alterovitz, R. J. W. III, and C. Rucker, "Computational analysis of design parameters for a bimanual concentric push-pull robot," in *Proceedings of The 15th Hamlyn Symposium on Medical Robotics 2023*, 2023, pp. 19–20.
- [23] P. L. Anderson, R. J. Hendrick, M. F. Rox, and R. J. Webster, "Exceeding traditional curvature limits of concentric tube robots through redundancy resolution," *The International Journal of Robotics Research*, vol. 43, pp. 53 – 68, 2023.